Available online at www.sciencedirect.com
SCIENCE DIRECT®
Chemical Physics Letters 411 (2005) 181–185
CHEMICAL PHYSICS LETTERS
www.elsevier.com/locate/cplett

Why is lead dioxide metallic?

David J. Payne [a], Russell G. Egdell [a,*], Wang Hao [b], John S. Foord [b], Aron Walsh [c], Graeme W. Watson [c]

[a] Department of Chemistry, Inorganic Chemistry Laboratory, South Parks Road, Oxford OX1 3QR, UK
[b] Department of Chemistry, Chemistry Research Laboratory, Mansfield Road, Oxford OX1 3TA, UK
[c] Department of Chemistry, University of Dublin, Trinity College, Dublin 2, Ireland

Received 6 May 2005; in final form 6 June 2005
Available online 29 June 2005

Abstract

The electronic structure of lead dioxide (PbO_2) has been studied by high resolution valence band X-ray photoelectron spectroscopy and electron energy loss spectroscopy, supported by band structure calculations carried out within the framework of density functional theory. The metallic nature of PbO_2 is shown to arise from occupation of conduction band states above the Fermi level of stoichiometric PbO_2, probably arising from oxygen vacancy defects. Strong satellites are observed in core level photoemission spectra at an energy consistent with the plasmon frequency observed in electron energy loss spectra.

Lead dioxide (PbO_2) is of ubiquitous importance as the medium for storage of chemical energy in lead acid batteries [1]. Despite the significant environmental problems associated with these batteries, they continue to dominate the road transport industry, with a world market of the order of $30 billion per annum. It is not always recognised that PbO_2 is a metallic conductor [2,3], but the ability of lead acid batteries to deliver the high currents necessary to drive the starter motor for an internal combustion engine is crucially dependent on the low resistance of the cathode coating [4,5]. The reason *why* PbO_2 is metallic remains a matter of conjecture. Band structure calculations have suggested that the metallic behaviour is an intrinsic property of stoichiometric β-PbO_2 due to overlap of the Pb 6s conduction band with the valence band of O 2p states [6]. On the other hand, it is known that the carrier concentration varies with preparation conditions in a way suggestive of defect-induced conductivity [7]. Here, we report valence band photoelectron spectra of β-PbO_2, which in combination with density functional calculations, demonstrate unambiguously that metallic behaviour arises from population of electronic states above the top of the main O 2p valence band. These carriers must be introduced by defects.

Photoemission spectroscopy is a workhorse technique for investigation of filled electronic states in solids. The short path length of photoelectrons excited with far UV radiation necessitates rigorous surface preparation procedures if experiments are to yield meaningful results. Much longer photoelectron path lengths are found under soft X-ray excitation and photoemission experiments conducted using this higher energy radiation are more tolerant of imperfect surface preparation. Thus, X-ray photoemission spectroscopy (XPS) is much better suited than ultraviolet photoemission spectroscopy (UPS) to the study of valence band states in polycrystalline samples of the sort found in many technological applications. However, the cross-sections for ionisation of valence states with soft X-rays are much smaller than at lower vacuum UV photon energies [8]. It is therefore a major technical challenge to use X-ray photoemission to study the exceedingly weak features arising from

* Corresponding author. Fax: +44 0 1865272690.
E-mail address: russ.egdell@chem.ox.ac.uk (R.G. Egdell).

0009-2614/$ - see front matter © 2005 Elsevier B.V. All rights reserved.
doi:10.1016/j.cplett.2005.06.023

occupation of the conduction band in materials such as PbO_2 and SnO_2. Despite the enormous technological importance of PbO_2 we are unaware of any previous attempts to study conduction band states by photoemission. Here we address this challenge using an XPS system incorporating a high throughput analyser, high intensity X-ray source and parallel electron detection system.

Films of β-PbO_2 with the tetragonal rutile structure were deposited on polished Pt substrates by anodic oxidation of solutions of 0.4 M $Pb(NO_3)_2$ in 0.1 M HNO_3. A current density of around 10 mA cm^{-2} and a deposition temperature of 60 °C gave optimal phase purity, with strong reflections in X-ray diffraction associated with tetragonal β-PbO_2 and minimal intensity in orthorhombic α-PbO_2 reflections [9,10]. The nominal film thickness was 15 μm. The films were rinsed in ultrapure water and dried at 100 °C. High-resolution X-ray photoemission spectra were measured in a Scienta ESCA 300 spectrometer operated under the aegis of the National Centre for Electron Spectroscopy and Surface Analysis (NCESS) at Daresbury Laboratory (UK). This incorporates a rotating anode Al Kα X-ray source, a 7 crystal X-ray monochromator and a 300 mm mean radius spherical sector electron energy analyser with channel plate electron detection system. The effective instrument resolution was 350 meV. β-PbO_2 has only limited thermal stability and it is not possible to use standard procedures such as argon ion bombardment and high temperature annealing in UHV to prepare 'clean' surfaces. However due to the strongly oxidising nature of PbO_2, it was found that surfaces were often spontaneously free of adventitious carbon contamination even without in situ pre-treatments. Annealing at temperatures up to 230 °C in UHV was also possible without loss of integrity of the rutile phase. Valence band spectra were typically accumulated over time periods of the order of 4 h, giving total accumulated counts around 15 000 on the strongest peak in the O 2p valence band and around 500 on the conduction band states. Electron energy loss spectra were measured in a home-built spectrometer incorporating a PSP ELS 100 low energy electron source and a VSW 100 mm spherical sector analyser incorporating a channel plate electron detection system.

Fig. 1a shows the valence band X-ray photoemission spectrum of a PbO_2 film which has been annealed in situ at 230 °C for 1 h. The spectrum is dominated by the O 2p valence band which contains three features, labelled I–III in the figure. The metallic nature of PbO_2 is demonstrated by the fact that the spectrum is truncated by a weak but sharp Fermi edge whose position is coincident with that of a metallic silver sample used to calibrate the spectrometer. The Fermi edge was always found to lie well above the top of the main valence band peak I. However, both the intensity of the Fermi edge cutoff

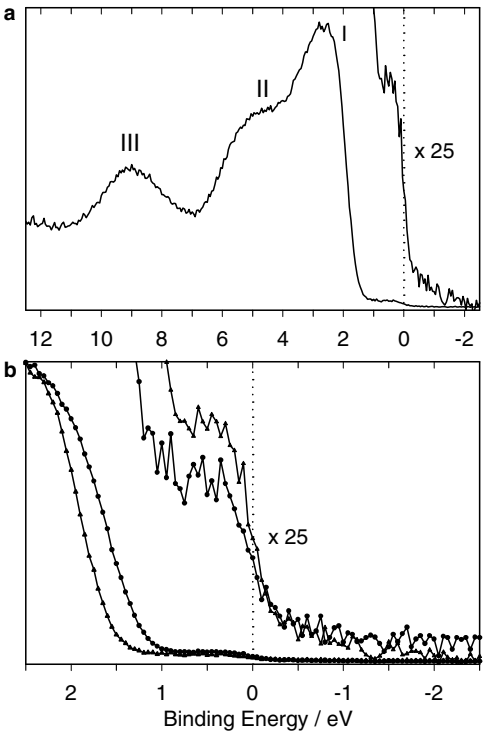

Fig. 1. (a) Valence band X-ray photoemission spectrum of β-PbO_2 thin film that has been subject to in situ annealing at 230 °C for 1 h. (b) Comparison of structure in vicinity of Fermi energy for an as-presented β-PbO_2 sample (filled circles) and sample heated in situ at 230 °C (filled triangles) as in (a). Note the increased intensity of the Fermi edge and the shift of the valence band edge to high binding energy as a consequence of annealing in UHV.

and its position relative to the valence band edge were strongly dependent on the nature of in situ treatments, as illustrated in Fig. 1b. These observations demonstrate in a simple way that the metallic behaviour arises from variable filling of a conduction band which lies above the main valence band. Of course all binding energies are referenced to the Fermi energy and the shifts in the Fermi level within the conduction band are manifest in terms of shifts in the valence band edge to higher binding energy with increasing filling of the conduction band. The downward shift of the valence band edge of 0.26 eV evident in Fig. 1b and the observed increase in the intensity of the Fermi edge as a result of in situ annealing at 230 °C may be analysed in terms of the free-electron expressions for the Fermi energy E_F and the density of states at the Fermi energy $N(E_F)$:

$$E_F = \frac{\hbar^2}{2m}(3\pi^2 n)^{2/3},$$

$$N(E_F) = \frac{1}{2\pi^2}\left(\frac{2m^*}{\hbar}\right)^{1/2}(3\pi^2 n)^{1/3},$$

where n is the electron concentration and m^* is the electron effective mass. The increase in the density of states at the Fermi energy by a factor of 1.2 implies an increase of the conduction electron concentration by a factor of

1.9. Taken in conjunction with the shift in the valence band edge and assuming that $m^* = 0.8m_0$ (where m_0 is the electron rest mass) [7] this variation allows us to deduce that the carrier concentration increases from 1.1×10^{21} to 2.0×10^{21} cm^{-3} as a consequence of annealing at 230 °C in UHV.

For comparison with the experimental data, density functional theory as embodied in the Vienna ab initio simulation package (VASP) [11,12] was used to calculate the electronic structure of β-PbO_2. The crystal wave functions were expanded in terms of a plane wave basis set using periodic boundary conditions with a plane wave cutoff of 500 eV and a k-point grid density of $4 \times 4 \times 6$. The generalised gradient approximation (GGA) parameterisation of Perdew et al. [13] was used with the projector augmented wave method [14] employed to represent the valence–core interactions (Pb: [Xe], O: [He]). These fixed core states were generated from all-electron scalar relativistic calculations. The calculated lattice parameters were $a = b = 5.083$ Å and $c = 3.453$ Å, representing small deviations of only +2.5% and +2.0%, respectively, from experimental values.

The calculated total and partial densities of states are shown in Fig. 2. The occupied valence band is seen to contain three main features, corresponding to the three peaks I–III seen in the experimental spectrum. The valence band states all have significant O 2p character. However, there is pronounced mixing between both the Pb 6s and 6p states and the O 2p states: in fact the states in the most tightly bound band (III) are of almost equal Pb 6s and O 2p atomic character. Mixing with Pb 6p states is essentially confined to band II. In our calculations β-PbO_2 emerges as a semi-metal: the density of states drops to zero at the Fermi energy, but without a significant energy gap. The lowest conduction band is of strongly mixed Pb 6s–O 2p atomic character and in fact there is more 6s character in the occupied states than in the empty states. The metallic behaviour of PbO_2 must arise from occupation of the strongly hybridised lowest conduction band state, which would be empty in stoichiometric PbO_2. The simplest way in which it is possible to envisage population of the conduction band is as a result of oxygen deficiency. Assuming that each vacancy is doubly ionised, the maximum carrier concentration of around 2.0×10^{21} cm^{-3} found in the present work equates to an oxygen deficiency parameter $x = 0.042$, as defined by the formula PbO_{2-x}.

The screening response of the mobile conduction electrons in β-PbO_{2-x} has a profound influence of the structure of core photoemission lines. Fig. 3 shows the $4f_{7/2}$ line for non-metallic α-PbO (chosen as a reference material and cleaned in situ by heating a pellet at 400 °C for 1 h) along with the corresponding peak for β-PbO_{2-x}. In agreement with Thomas and Tricker [15] we find a shift to low binding energy on oxidation from PbO to PbO_2. A shift of this sort is of course at variance with

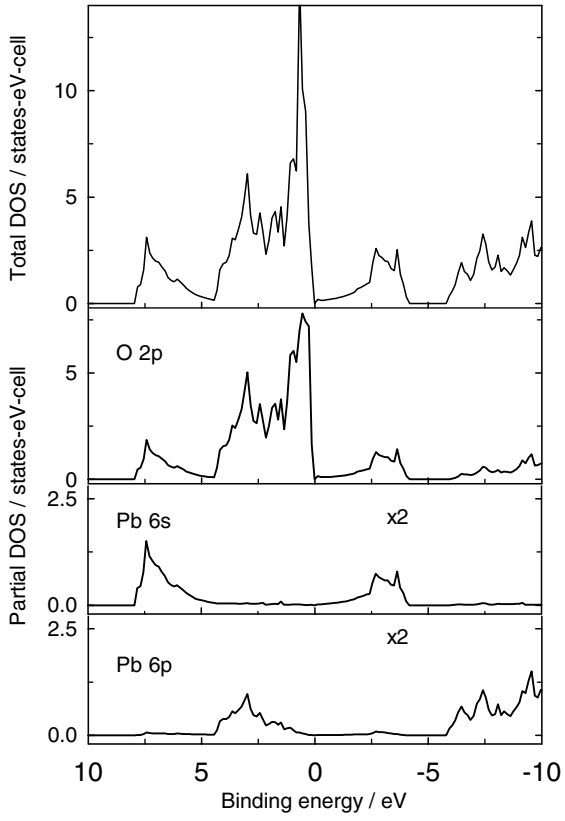

Fig. 2. The total and partial densities of states for β-PbO_2 derived from density functional calculations.

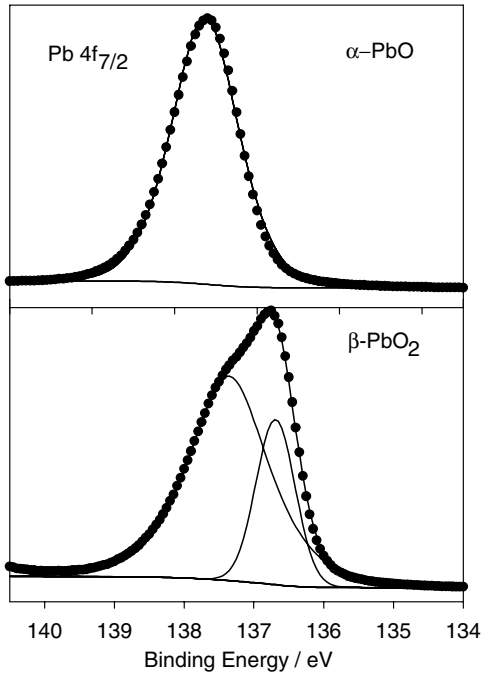

Fig. 3. The Pb $4f_{7/2}$ core level peak for α-PbO and for 'as presented' β-PbO_2. Note the strong satellite structure in the latter.

the simple idea that binding energies should increase with increasing oxidation state. The core line for atomically clean α-PbO can be fitted with a single Voigt component. However, the lineshape for β-PbO_{2-x} is more complex. The overall spectral profile fits to a relatively narrow peak at low binding energy and a broader 'satellite' with a dominantly Lorentzian lineshape at higher binding energy. The 'satellite' actually carries greater spectral weight than the low binding energy peak. The separation between the two peaks accords with the plasmon energy as measured in separate reflection electron energy loss experiments. For example, Fig. 4 shows an electron energy loss spectrum measured under 100 eV excitation for an as-presented thin film sample. The energy of the loss peak –0.65 eV – is very close to the separation between the 'main' peak and the satellite seen in Fig. 3.

In a simple free electron model, the plasmon energy E_p varies with carrier concentration n as [16]

$$E_p = \hbar\sqrt{\frac{ne^2}{m^*\varepsilon(\infty)\varepsilon_0}},$$

where m^* is the electron effective mass, $\varepsilon(\infty)$ is the background dielectric constant, e is the electron charge and ε_0 is the permittivity of free space.

In agreement with assignment of the satellites to plasmon structure, the satellite energy was found to undergo pronounced variations with in situ annealing treatments. Thus, the satellite energy increases from 0.69 eV for an as-presented sample to 1.00 eV after annealing at 210 °C for 1 h and to 1.02 eV after further annealing at 230 °C (Fig. 5). The overall increase in the plasmon energy between Figs. 3 and 5b implies a doubling in the carrier concentration, in agreement with the increase in the intensity of the conduction band seen in Fig. 1.

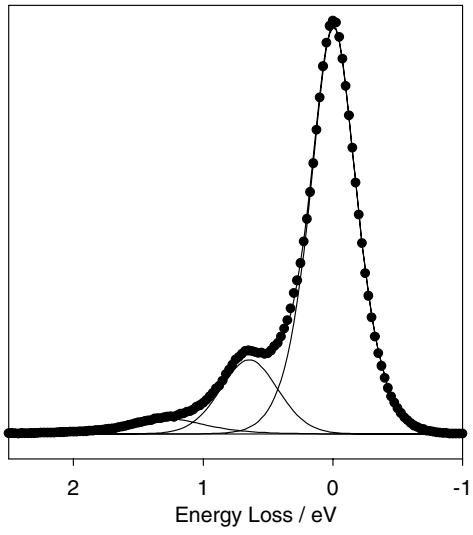

Fig. 4. Electron energy loss spectrum of as-presented PbO_2 thin film excited with 100 eV electron beam showing single and double plasmon losses.

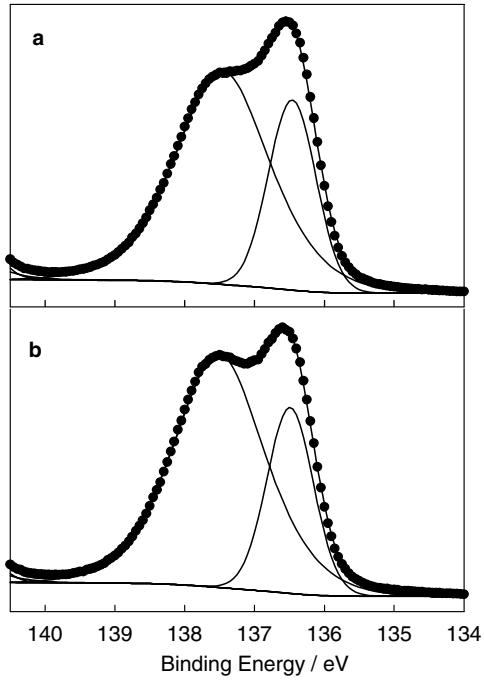

Fig. 5. The Pb $4f_{7/2}$ core level peak for β-PbO_2 annealed for 1 h in UHV at (a) 200 (b) 230 °C. Note the small increase in the energy of the high binding energy satellite after the higher temperature anneal.

The observed energies of the plasmon satellites suggests that $\varepsilon(\infty) = 3.8$.

The plasmon satellites observed in the present work are much stronger than those found in core photoemission spectra of conventional metals such as Na, Mg and Al [17]. However, it is known that the probability of intrinsic plasmon excitation should vary as $n^{-1/3}$ (where again n is the carrier concentration), so strong satellite structure is expected in dilute electron gas systems [18]. Similarly strong plasmon satellites have been observed previously in core XPS of Sb-doped SnO_2 [19,20] and Sn-doped In_2O_3 [21]. A somewhat puzzling aspect of the satellite structure is that only a single plasmon satellite is observed: for the conventional metals alluded to above, multiple plasmon satellites are found. In electron energy loss spectroscopy, loss features at both E_{sp} and $2E_{sp}$ are also observed due to sequential inelastic scattering. We must conclude that the dominant mechanism for plasmon excitation in XPS is *not* via extrinsic sequential scattering: rather single plasmon excitation appears as an intrinsic part of the screening response in dilute electron gas metals.

In summary, we have shown that the metallic nature of β-PbO_2 arises from partial occupation of a conduction band of strongly hybridised Pb 6s–O 2p states. The charge carriers arise from oxygen vacancy defects and the carrier concentration is strongly dependent upon sample pre-treatments. The screening response of the mobile conduction electrons produces strikingly strong satellites in core XPS.

References

[1] R.M. Dell, D.A.J. Rand, Understanding Batteries, Royal Society of Chemistry, Cambridge, 2001.
[2] A.A.K. Vervaet, D.H.I. Baert, Electrochim. Acta 47 (2002) 3297.
[3] T. Kimura, A. Ishiguro, Y. Andou, K. Fujita, J. Power Sources 85 (2000) 149.
[4] W. Mindt, J. Electrochem. Soc. 116 (1969) 1076.
[5] P.T. Moseley, J.L. Hutchinson, M.A.M. Bourke, J. Electrochem. Soc. 129 (1982) 876.
[6] M. Heinemann, H.I. Terpstra, C. Haas, R.A. de Groot, Phys. Rev. B 52 (1995) 11740.
[7] J.P. Pohl, G.L. Schlectriemen, J. Appl. Electrochem. 14 (1984) 521.
[8] J.J. Yeh, I. Lindau, Atom Data Nucl. Data 32 (1985) 1.
[9] A.B. Velichenko, R. Amadelli, A. Benedetti, D.V. Girendko, S.V. Kovalyov, F.I. Danilov, J. Electrochem. Soc. 149 (2002) C445.
[10] S. Abaci, K. Pekmez, T. Hõkelek, A. Yildiz, J. Power Sources 88 (2000) 232.
[11] G. Kresse, J. Hafner, Phys. Rev. B 49 (1994) 14251.
[12] G. Kresse, J. Furthmuller, Comput. Mater. Sci. 6 (1996) 15.
[13] J.P. Perdew, K. Burke, M. Ernzerhof, Phys. Rev. Lett. 77 (1996) 3865.
[14] P.E. Blöchl, Phys. Rev. B 50 (1994) 17953.
[15] J.M. Thomas, M.J. Tricker, J. Chem. Soc., Faraday II 70 (1974) 329.
[16] C. Kittel, Introduction to Solid State Physics, Wiley, New York, 1996.
[17] P. Steiner, H. Hõchst, S. Hüfner, in: L. Ley, M. Cardona (Eds.), Photoemission in Solids II: Case Studies, Topics in Applied Physics, 27, Springer, Berlin, 1979, p. 349.
[18] J.N. Chazalviel, M. Campagna, G.K. Wertheim, H.R. Shanks, Phys. Rev. B 16 (1997) 697.
[19] R.G. Egdell, J. Rebane, T.J. Walker, D.S.L. Law, Phys. Rev. B 59 (1999) 1792.
[20] R.G. Egdell, T.J. Walker, G. Beamson, J. Electron. Spectrosc. Relat. Phenom. 128 (2003) 59.
[21] V. Christou, M. Etchells, O. Renault, P.J. Dobson, O.V. Salata, G. Beamson, R.G. Egdell, J. Appl. Phys. 88 (2000) 5180.